

Investigation of structure and properties of low alloy steel obtained by wire arc additive manufacturing under various fluxes

G E Trekin

Ural Federal University named after the First President of Russia B N Yeltsin, Nizhniy Tagil Technological Institute, 59, Krasnogvardeyskaya str, Nizhniy Tagil, 622000, Russia

E-mail: trekin1963@yandex.ru

Abstract. Wire arc additive manufacturing (WAAM) is vigorously explicating direction of mechanical engineering. When using submerged arc welding (SAW) it is possible to apply low-alloy steels with high efficiency and properties, that will allow to use it for manufacture of details and instrument. Microstructure, hardness, distribution of nonmetallic and chemical composition were investigated for SAW build up walls, in as-deposited condition, by low-alloy wire under fluxes with a different basicity. The characteristics of microstructure fixed by an optical microscopic metallography remain practically constant for all deposited weld metals. It is ferrite – martensite (bainite) structure, which has a high dispersibility. The exploration of hardness has shown formation of the partially quenched top with increased hardness and previous thermo- cyclic treated passes with lower hardness. When depositing SAW insignificant saturation of metal with silicium and manganese and a carbon drop occurs. The distribution of nonmetallics is most favorable for additive manufactured material under neutral and basic fluxes. As a result, a comparative research of fluxes was conducted, allowing to make a choice for additive manufacturing of low-alloy work pieces.

1. Introduction

The additive technologies allow to manufacture work pieces with the improved properties and ensure their economic expediency when the shape is irregular [1]. Most of the reviews do not give attention to low-alloy steels and submerged arc welding (SAW) [2, 3], because there is no its robotized equipment. The works using WAAM for workspaces from low-carbon and low-alloy steels, apply gas-metal arc welding [4, 5, 6]. The structure forming of deposited metal at arc additive manufacturing occurs at a crystallization and consequent technologically inevitable (automatic) thermo- cyclic treatment (ATCT) from the last passes to the previous ones [7, 8]. Thus ferrite – martensite (bainite) structure of different ratio of ferrite with a different morphology (acicular, polygonal granular etc.) is formed, and the martensite -austenitic constituents also detected [4]. The geometrical sizes of a building joint are determined by a diameter of a wire, welding parameters and surface-tension of a melt [9]. The chemical composition also depends on welding mode and saturation/expulsion of alloy elements in the process of chemical interaction between depositing metal and protective medium [10]. The set of metal properties obtained by arc additive manufacture is attractive enough for its use in industry. The metal has high level of residence to brittle fracture [11].



2. Materials and methods

The wall-shaped work pieces were built-up by means of SAW equipment ADC -1250 SF with a wire 30KhaGSA (Table 5) at diameter of 3 mm and standard mode (Table 1) under fluxes AN - 348A, FSA ChTA 650 -20/80 and UF-01 (Table 2–4), number of passes 51, as a base metal a low carbon steel plate with the thickness of 20 mm was used. The exploration of chemical composition was executed on Q2 - ION device.

Table 1. Submerget arc welding parameters.

Current (A)	Voltage (V)	Welding speed (m/hr)	Wire feed speed (m/min)	Electrode stick out (mm)	Inter-pass time (min)
540	44	40	0.9	30	50–60

Table 2. The nominal chemical composition (mass. %) and basicity index (BI_f) of AN-348A flux.

SiO ₂	MnO	MgO	CaF ₂	CaO	Al ₂ O ₃	Fe ₂ O ₃	S	P	BI _f
41–44	34–38	5–7.5	4–5.5	<6.5	<4.5	<2	<0.15	<0.12	0,75

Table 3. The nominal chemical composition (mass. %) and basicity index (BI_f) of FSA ChTA 650 -20/80 flux.

Al ₂ O ₃ + CaO+ MgO	Al ₂ O ₃	CaF ₂	BI _f
>40	>20	>22	1.2

Table 4. The nominal chemical composition (mass. %) and basicity index (BI_f) of UF -01 flux.

CaO+ MgO+ CaF ₂ +MnO	SiO ₂	CaF ₂	BI _f
>50	>20	>15	3.2

The metallographic study was performed with a Zeiss Observer D1m microscope running under Thixomet software. Etching was carried out with Nital (6 %) solution for 20 s at the room temperature. Hardness indentation were made using a DURA Jet testing machine by Rockwell C-method. The results were processed by means of Excel and MathCAD software.

3. Results and discussion

The shape of a single weld pass is crescent with a superficial weld penetration cog in the center. After a consequent deposit welding, pass by pass, a vertical wall of height 60–65 mm and width of 14–18 mm is formed without cracks. Because of low toughness of molten metal under flux, there is an increment of a thin layer with a thickness about 1 mm. The previous pass is remelted by 74 % and 1 mm thick strip remain here. The strip completely gets into a heat-affected zone and exposes to short thermal effect. After a deposit welding of consequent passes, there is triple remelting and auto thermo-cyclic treatment (ATCT) by short thermal heats with decreasing of maximal temperature from near melting point to a low tempering (Figure 1).

After SAW under fluxes AN-348A and FSA ChTA 650 -20/80 there remains about 40 % of carbon initially contained in a wire and about 60 % under a flux UF-01. The SAW building-up under all fluxes results in insignificant saturation of deposited metal with silicium. The significant saturation with manganese occurs only under flux AN-348A and FSA ChTA 650 -20/80 by 1.5 % and 0.79 %, for a flux UF-01 it is accordingly insignificant and makes about 0.2 %. The expulsion of a chromium is observed only for a flux AN-348A (table 5). Under fluxes AN-348A and FSA ChTA 650 -20/80 chemical composition with the least carbon content and greatest silicium and manganese content is formed. Under flux UF-01 – with the greatest carbon content and with the least silicium and manganese content is formed, with hardly varying of the chromium content.

The analysis of hardness distribution along the height of deposited metal showed, that the top passes have 16–32 % higher hardness in comparison with the bottom located passes, which passed auto thermo-cyclic treatment (figure 2, table 5).

The analysis of structure revealed a ferrite – martensite (bainite) structure in the top passes. It has a small volumetric fraction of ferrite for all investigated samples of a deposited metal, that stipulates higher hardness of the top pass. In bottom areas of a weld metal the fraction of ferrite was increased and dispersed perlite was most likely formed after high-temperature thermo – cyclic treatment affect.

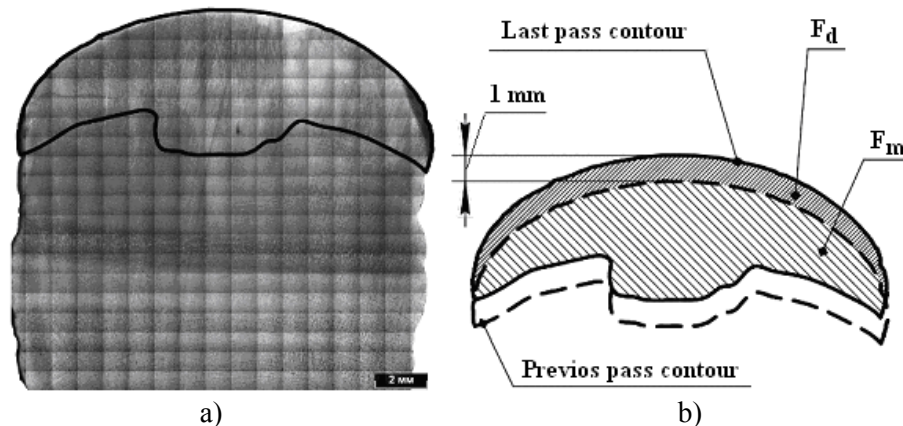


Figure 1. Wire arc additive manufactured wall formation (flux AN-348A).
a – transversal section, b – passes contours reconstruction;
 F_d – deposited metal area, F_m – melting area; MM = mm

Table 5. The chemical composition and hardness of deposited metal (DM) and wire.

Flux	contents of elements (mass. %)				Hardness (HRC) after:	
	C	Si	Mn	Cr	deposition	deposition and ATCT
Wire 30KhaGSA	0.34	0.97	0.81	0.75	–	–
AN-348A	0.13	1.15	2.31	0.56	31	26
FSA ChTA 650 -20/80	0.14	1.20	1.59	0.72	31	21
UF-01	0.21	1.04	1.02	0.79	26	19

The structure of metal deposited under the low basic flux has the greatest dispersibility (Figure 4).

The estimation of nonmetallics was fabricated at small ($\times 50$) and large ($\times 1000$) magnification. First of them characterize particulate contamination with rather big inclusions, which are formed mainly at a stage of interaction of hydro dynamical currents of metal and molten flux in a welding bosh. Second of them originate in a liquid and solid condition, they grow or can be dissolved mainly in a solid condition.

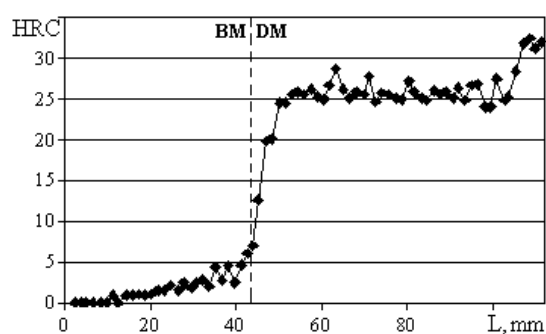


Figure 2. Hardness distribution (HRC) along wall height (L) (flux AN-348A):
BM – basemetal (initial plate);
DM – deposited weld metal.

The greatest inclusion volume fractioning during metal building up, deposited under the flux AN - 348A, is connected with its high saturation with oxygen. For flux FSA ChTA 650 -20/80 and UF-01 these magnitudes are less (Figure 5). The high fraction of big inclusions which got to polished section with the size from 30 up to $910 \mu\text{m}^2$ is more probably of more hampered conditions floating of

nonmetallics at the used conditions for fluxes AN - 348A and FSA ChTA 650 -20/80 if compare with flux UF-01 (Figure 4 b, d, f). At the large increase, the greatest fraction of conclusions up to $1 \mu\text{m}^2$ for fluxes FSA ChTA 650 -20/80 and UF-01 and the significant fraction of conclusions with the sizes from 1,5 up to $18 \mu\text{m}^2$ (Figure 4, d, f) is connected to distinctions in a melting temperature of fluxes. The interval of melting for welding fluxes strongly influences on an amount and aspect micro – flux contaminations, remaining in a weld metal. The components of a welding flux having a solidification point higher, than the weld metal are present in liquid metal of welding pool in the form of the smallest spherical particles and have time to be floated up from the pool before its crystallization. The acid and neutral fluxes have a melting temperature about $1350\text{--}1450 \text{ }^\circ\text{C}$, therefore the amount of micro – slag particles in metal of a weld is more than at the use of basic fluxes.

Formation of the melting contour shape is not absolutely favorable under all considered fluxes, as the central melting cog is formed, that can increase probability of forming interlayers cracks. Therefore it is necessary to achieve a melting contour approaching to a direct line without the central local melting. It can be achieved diffusing electromagnetic effects application, welding with the modulated current, other technological effects and changing SAW modes.

The obtained structure is capable to show high properties as the metal was remelted three times and because of a thin remaining strip exposes practically homogeneous consequent pulse thermal effect, that in combination with temperature monitoring between passes leads to a high homogeneity of structure, that is confirmed by a small scatter of hardness and chemical composition. The areas of initial changes of chemical composition and final partial ATCT are approximately identical and consist of 10–12 passes.

The fraction of rather large inclusions with its area of more than $300 \mu\text{m}^2$, if accepting particles as spherical, has the size of more than $19.5 \mu\text{m}$, makes 0.079 for AN - 348A; 0.095 for FSA ChTA 650 -20/80 and 0.074 for UF-01. It shows that the content level of relatively large nonmetallics a little bit higher for FSA ChTA 650 -20/80, but in general is of the same order, therefore it is difficult to identify the best flux from this parameter. The analysis of the particle sizes revealed at high magnification shows, that their sizes are less than the dangerous size of $10\text{--}20 \mu\text{m}$ ($38.5\text{--}78.5 \mu\text{m}^2$), defined in sources [12, 13], for all used fluxes, but their density in metal, deposited under the flux AN - 348A is many times more than when we use two other fluxes. The most favorable is considered to be a dispersed structure with an acceptable amount of non-metallic inclusions. Flux FSA ChTA 650 -20/80 is the most suitable for this criterion.

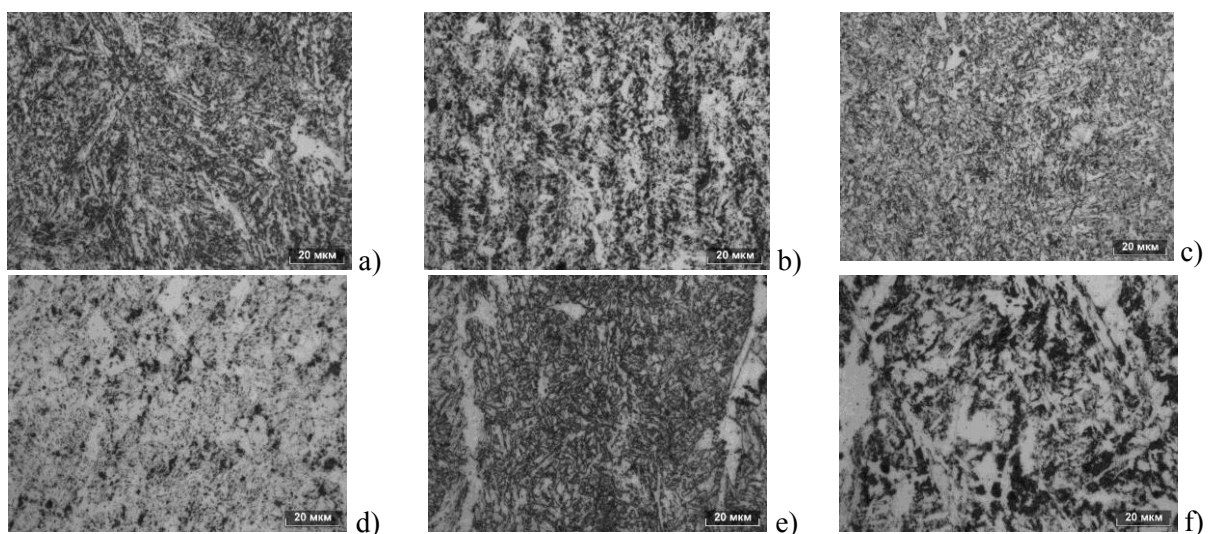


Figure 3. Optical micrographs of deposited weld metal.

flux: a, b- AN-348A; c, d - FSA ChTA 650 -20/80; e, f - UF -01
a, c, e – after deposition; b, d, f - after deposition and ATCT; scale in μm

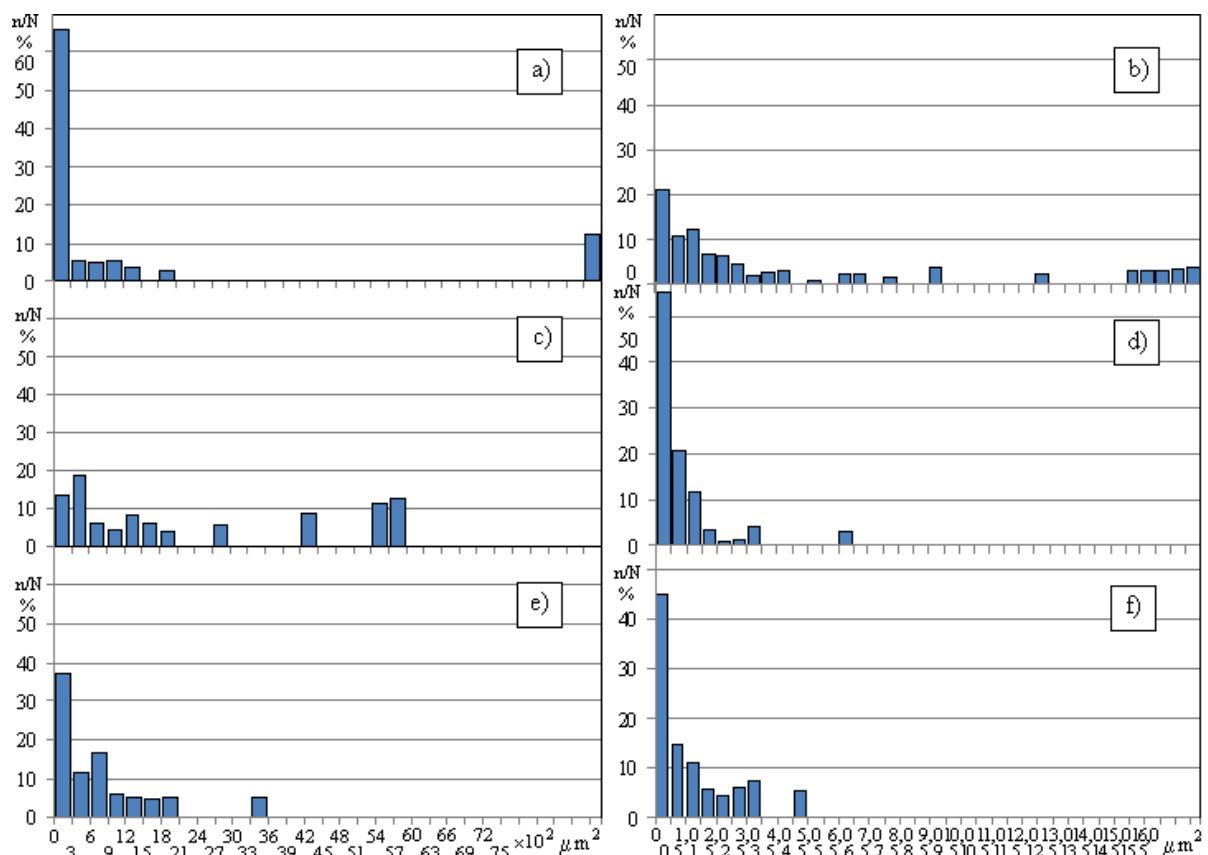
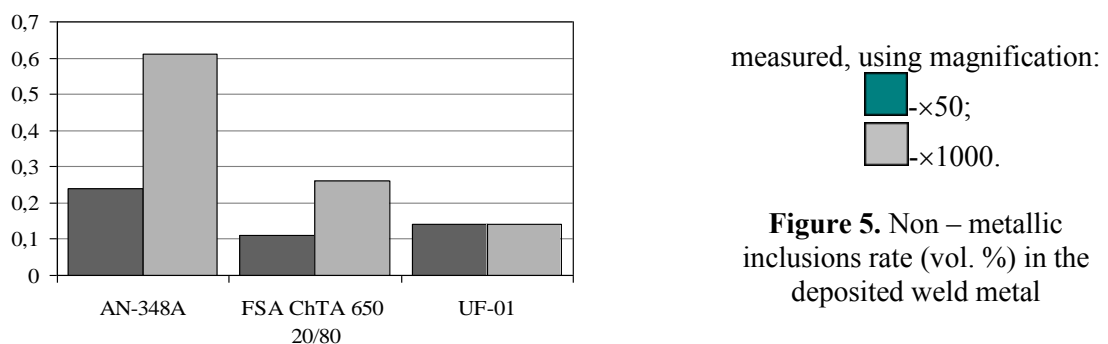


Figure 4. Histograms of the distributions non-metallic inclusions by area in the deposited weld metal. flux: a, b - AN-348A; c,d - FSA ChTA 650 -20/80; e,f - UF -01 measured, using magnification: a, c, e - $\times 50$; b, d, f - $\times 1000$



measured, using magnification:

 ■ $\times 50$;
 ■ $\times 1000$.

Figure 5. Non – metallic inclusions rate (vol. %) in the deposited weld metal

4. Summary

Thus, in the additive manufacturing of SAW under a flux by a wire with a diameter of 3 mm, using standard modes, a wall with a thickness of 14–18 mm forms. It has a high homogeneity and dispersibility of structure, except of the initial and final sections with the width of approximately the same as the thickness of the wall. When using 30KhaGSA wire under a layer of fluxes AN - 348A and FSA ChTA 650 -20/80 chemical composition with the least carbon content and greatest silicium and manganese content is formed. And under the flux UF-01 – with the greatest carbon content and with the least silicium and manganese content is formed, with hardly varying of the chromium content. The deposited metal has martensite – ferrite structure after a weld deposition, which stipulates higher hardness of the top passes. In bottom passes, hardness of 19 to 26 HRC is formed, which is stipulated

with the growth of ferrite fraction, formation of a dispersible pearlite and tempering of a martensite because of auto thermo – cyclic treatment. The greatest contamination with non-metallic inclusions has metal, deposited under the flux AN - 348A and the least – under UF-01. Based on the results of the research flux FSA ChTA 650 -20/80 is recommended for the use. It is also necessary to improve the weld deposition technology, to remove a weld penetration cog in the center of the pass.

References

- [1] Cunningham C R, Wikshaland S, Xu F, Kemakolam N, Shokrani E, Dhokia V and Newman S T 2017 Cost modelling and sensitivity analysis of wire and arc additive manufacturing *Procedia Manufacturing* vol **11** pp 650–7
- [2] Williams S W, Martina F, Addison A C, Ding J, Pardal G and Colegrove P 2016 Wire + Arc Additive Manufacturing *Materials Science and Technology* vol **32** no **7** pp 641–7
- [3] Wu B, Pan Z, Ding D, Cuiuri D, Li H, Xu J and Norrish J 2018 A review of the wire arc additive manufacturing of metals: properties, defects and quality improvement *Journal of Manufacturing Processes* vol **35** pp 127–39
- [4] Rodrigues T A, Duarte V, Avila J A, Santos T G, Miranda R M and Oliveira J P 2019 Wire and arc additive manufacturing of HSLA steel: Effect of thermal cycles on microstructure and mechanical properties *Additive Manufacturing* vol **27** pp 440–50
- [5] Nemani A V, Ghaffari M and Nasiri A 2020 Comparison of microstructural characteristics and mechanical properties of shipbuilding steel plates fabricated by conventional rolling versus wire arc additive manufacturing *Additive Manufacturing* vol **32** 101086
- [6] Rafieezad M, Ghaffari M, Nemani A V et al 2019 Microstructural evolution and mechanical properties of a low-carbon low-alloy steel produced by wire arc additive manufacturing. *Int. J. Adv. Manuf. Technol* **105** pp 2121–34
- [7] Xiong J, Li R, Lei Y and Chen H 2018 Heat propagation of circular thin-walled parts fabricated in additive manufacturing using gas metal arc welding *J. of Materials Processing Tech.* **251** pp 12–9
- [8] Ding D, Pan Z, Cuiuri D, Li H, Duin S and Larkin N 2016 Bead modelling and implementation of adaptive MAT path in wire and arc additive manufacturing *Robotics and Computer-Integrated Manufacturing* **39** pp 32–42
- [9] Rios S, Colegrove P A, Martina F and Williams S W 2018 Analytical process model for wire + arc additive manufacturing *Additive Manufacturing* **21** pp 651–7
- [10] Kanjilal P, Pal T K and Majumdar S K 2006 Combined effect of flux and welding parameters on chemical composition and mechanical properties of submerged arc weld metal *Journal of Materials Processing Technology* **171** pp 223–31
- [11] Shassere B, Nycz A, Noakes M V, Masuo C and Sridharan N 2019 Correlation of Microstructure and Mechanical Properties of Metal Big Area Additive Manufacturing. *Appl. Sci* **9** 787
- [12] Krivonosova E A and Belinin D S 2017 Transformation non-metallic inclusions in steels after plasma heating. *Bulletin of PNRPU Mechanical engineering, material science* vol **19** no **1** pp 58–77
- [13] Krivonosova E A 2016 The features of affecting non-metallic phases on deformation behavior weld deposited layers. *Bulletin of PNRPU. Mechanical engineering, material science* vol **18** no **1** pp 189–24